



ELSEVIER

Contents lists available at ScienceDirect

Materials Letters

journal homepage: www.elsevier.com/locate/matlet

A rare diarboxylate and N-oxide/H₂O bridged metal-organic framework with nickel(II)-oxide octahedral chains: synthesis, crystal structure, and magnetic properties with theoretical investigations on the exchange mechanism

Bing An^a, Yan Bai^{a,b,*}, Jun-Li Wang^a, Dong-Bin Dang^{a,*}^a Henan Key Laboratory of Polyoxometalate Chemistry, Institute of Molecular and Crystal Engineering, School of Chemistry and Chemical Engineering, Henan University, Kaifeng 475004, P.R. China^b State Key Laboratory of Coordination Chemistry, Nanjing University, Nanjing 210093, P.R. China

ARTICLE INFO

Article history:

Received 29 September 2014

Accepted 22 November 2014

Available online 2 December 2014

Keywords:

Nickel(II)

Metal chain

Co-ligands

Crystal structure

Magnetic properties

ABSTRACT

One 3D metal-organic framework $\{[\text{Ni}_2(1,4\text{-NDC})_2(4,4'\text{-dpdo})(\text{H}_2\text{O})] \cdot 3\text{H}_2\text{O}\}_n$ **1** (1,4-H₂NDC = 1,4-naphthalenedicarboxylate acid and 4,4'-dpdo = 4,4'-Dipyridyl-N,N'-dioxide) has been hydrothermally synthesized and well-characterized. Polymer **1** arranges in the 1¹O¹ fashion. The hexacoordinated Ni(II) centers are triply bridged by two 1,4-NDC²⁻ carboxylate group plus μ -4,4-dpdo or μ -H₂O to form an alternating chain. Each metal chain is cross-connected to four other chains to shape a 3D network. Magnetic studies show that **1** exhibits dominant ferromagnetic interactions with intrachain alternating antiferromagnetic/ferromagnetic interactions.

© 2014 Elsevier B.V. All rights reserved.

1. Introduction

Materials with switchable physical properties in the solid state are of considerable interest in both applied and fundamental points of view. Molecular materials are chemically flexible and thus good candidates to reach this goal [1,2]. The research on molecular magnetic systems has witnessed a rapid development for decades, aimed at clarifying magnetic phenomena, revealing magnetostructural correlations and constructing new magnetic materials with potential applications such as magnetic sensors, magnetic switchers and multifunctional magnetic devices [3–5]. Since purely 1D magnetic systems does not exhibit long-range order at finite temperature, the interchain interactions are crucial on the cooperative magnetic properties of the materials [6].

Up to now, the design and synthesis of polynuclear and chain-like polymers with predictable magnetic properties are still a challenge owing to many factors, especially the connection nodes of organic ligands. Carboxylate can efficiently mediate either ferromagnetic (FM) or antiferromagnetic (AFM) coupling through various coordinating modes, as well as they can be used as the connection between

magnetic moment carriers (metal nodes) with the interacting range to form robust MOFs exhibiting long-range magnetic ordering [7,8]. Therefore, the employment of carboxylate ligands can make contributions to efficient magnetic exchange between neighboring magnetic carriers, which has been proven to be a meaningful method to create molecular magnets. 4,4'-Dipyridyl-N,N'-dioxide (4,4'-dpdo) as a good candidate for assembly of magnetic materials can offer a variety of magnetic interactions due to its versatile bridging modes [9,10]. Recently, we have successfully obtained some MOFs derived from 1,4-naphthalenedicarboxylate acid (1,4-H₂NDC) and 4,4'-dpdo, which manifest interesting optical and/or magnetic properties [11–13]. Herein we report the structure and magnetic property of one 3D MOFs $\{[\text{Ni}_2(1,4\text{-NDC})_2(4,4'\text{-dpdo})(\text{H}_2\text{O})] \cdot 3\text{H}_2\text{O}\}_n$ **1** which consists of 1D metal chains with two kinds of triple bridge, which exhibiting an intrachain ferromagnetic coupling with long-range magnetic ordering. And a theoretical study was also performed to estimate the exchange coupling constants and to explore the mechanism of the magnetic property of the system.

2. Experimental

2.1. Synthesis

The polymer was synthesized by hydrothermal methods. A mixture of Ni(NO₃)₂ · 6 H₂O (0.3 mmol), 1,4-H₂NDC (0.1 mmol), 4,4'-dpdo (0.1 mmol), NaOH (0.2 mmol) and distilled water

* Corresponding authors at: Henan Key Laboratory of Polyoxometalate Chemistry, Institute of Molecular and Crystal Engineering, School of Chemistry and Chemical Engineering, Henan University, Kaifeng 475004, P.R. China.
Tel.: +86 371 23881589; fax: +86 371 23881589.

E-mail addresses: baiyan@henu.edu.cn (Y. Bai), dangdb@henu.edu.cn (D.-B. Dang).

(15 mL) was stirred for 1 h. The mixture was then transferred to a 25 mL Teflon-lined steel autoclave and kept at 160 °C for five days under autogenous pressure. After the mixture had been slowly cooled down to room temperature, brown block crystals were obtained. Yield: ca. 69%. Anal. Calcd(%) for $C_{34}H_{28}Ni_2N_2O_{14}$: C, 50.67; H, 3.50; N, 3.48. Found: C, 50.74; H, 3.56; N, 3.43. IR (cm^{-1} , KBr pellet): 3435(w), 1592(vs), 1578(vs), 1511(w), 1471(s), 1418(s), 1372(s), 1259(w), 1228(m), 1180(m), 1025(w), 839(m), 828(m), 795(m), 779(w), 768(m), 557(m).

3. Results and discussion

3.1. Description of the crystal structure of polymer **1**

There are two crystallographically independent nickel(II) centers in **1** and both of them have a distorted octahedral geometry with the O_6 donor set (Fig. 1). All the equatorial plane oxygen donors are from the 1,4-NDC $^{2-}$ ligands. The Ni–O bond lengths are in the range of 2.022(8)–2.125(6) Å for Ni(1)–O and 1.997(9)–2.118(6) Å for Ni(2)–O. Each 1,4-NDC $^{2-}$ ligand binds four Ni(II) ions through two μ_2 - η_1 : η_1 carboxylates in a *syn-syn* fashion.

In **1**, O(2) and O(1 W), the opposite corner-sharing oxygen atoms in the axial positions, are alternate linkage of NiO $_6$ octahedra to generate a [Ni(1)–O(1 W)–Ni(2)–O(2)] $_n$ inorganic chain (Fig. 2). The Ni ··· Ni distances in the alternate chain through the μ_2 -O linkages are 3.57 Å and 3.53 Å; two kinds of Ni ··· Ni ··· Ni angles are 175.1° and 171.0°, respectively, which indicates that the chain is almost collinear. Each chain is cross-connected to four other chains through 1,4-NDC $^{2-}$ ligands to shape a 3D network (Fig. 3). The packing of **1** arranges in the I $^1O^1$ fashion with the adjacent interchains separations approach to 11 Å. 4,4'-Dpdo ligand is attached in an unusual μ -4,4 bridging mode, which is important in the formation of inorganic chain but has no contribution to construct the 3D framework. Topologically, the overall framework of **1** can be represented as six-connected net with a short Schläfli symbol of (4 12 .6 3).

3.2. X-ray powder diffraction and scanning electron microscope (SEM)

The peak positions of the X-ray powder diffraction pattern of **1** are in good agreement with the simulated, demonstrating the phase purity of the products (Fig. S1). The SEM images of the samples show that the crystals have smooth surfaces and conspicuous crystal faces, demonstrating the homogeneity of the product (Fig. 4).

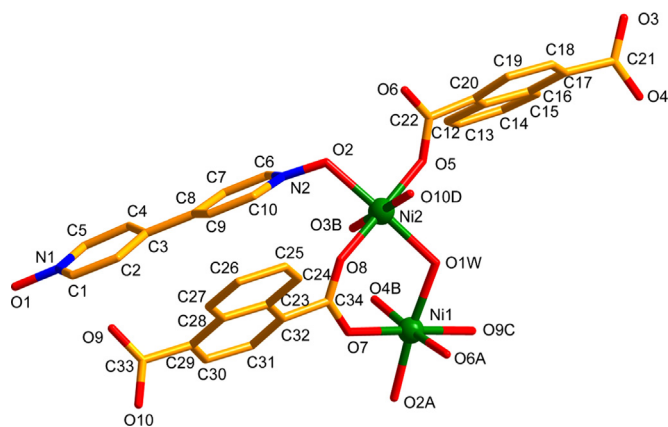


Fig. 1. A view of **1** with the atom numbering scheme. All the H atoms and lattice solvents are omitted for clarity. Symmetry codes: A, $x, -y, 1/2+z$; B, $1/2+x, 1/2-y, 1/2+z$; C, $-1/2+x, 1/2+y, z$; D, $-1/2+x, -1/2-y, -1/2+z$.

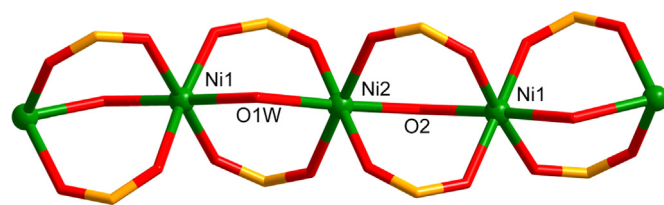


Fig. 2. Representation of alternating nickel(II) triply connected in polymer **1**.

3.3. Magnetic properties

The magnetic susceptibility of **1** under 1000 Oe in the range of 1.8–300.0 K is shown in Fig. 5. The room temperature $\chi_M T$ value is 3.74 $cm^3 mol^{-1} K$ per Ni $_2$ unit. When the temperature is lowered, $\chi_M T$ value remains nearly constant until 50 K, and upon further cooling, the $\chi_M T$ value rapidly increases to a maximum of 62.73 $cm^3 mol^{-1} K$ at 18 K and then quickly drops. The data fitting of Curie-Weiss law in the range of 100–300 K gives $C=3.61 cm^3 mol^{-1} K$ and $\theta=3.83 K$. This behavior evidently indicates the presence of intrachain ferromagnetic coupling interactions.

According to the structural characteristics, there are two types of intrachain magnetic exchange pathways corresponding to different linkages, J_1 and J_2 through μ_2 -O(1 W) and μ_2 -O(2) with alternate arrangement (Scheme S1). The $\ln(\chi T)$ versus T^{-1} plot is linear between 20 and 54 K supporting an anisotropic Heisenberg or Ising-like 1D character (Fig. S2). The low-temperature deviation from linearity may be due to a combination of field effect, finite-chain effect and weak interchain antiferromagnetic interactions. The linear $\ln(\chi T)$ versus T^{-1} relationship, which is theoretically deduced for 1D chains, is only a rough approximation for our chains [14].

To evaluate the magnetic interactions of the 1D alternating chain structures, the system may be magnetically handled as the alternating 1D Heisenberg Fisher model (Eq. (1)) based on the Hamiltonian (Eq. (2)). Meanwhile, we incorporate λ as a correction item which takes care of both the orbital contribution due to the presence of the interchain antiferromagnetic interaction [15]:

$$\chi_{\text{chain}} = \frac{Ng^2\beta^2 S(S+1)}{3k(T-\lambda)} \frac{1+u_1+u_2+u_1u_2}{1-u_1u_2} \quad (1)$$

$$\hat{H} = -J_1 \sum^N S_{2i} S_{2i+1} - J_2 \sum^N S_{2i+1} S_{2i+2} \quad (2)$$

where u is the well-known Langevin function defined as $u = \coth[J_i S(S+1)/kT - kT/J_i S(S+1)]$ ($i=1, 2$) with $S=1$. The model provides a good fit of the experimental data over the range 50–300 K, yielding $J_1/k_B=6.8 K$, $J_2/k_B=-2.7 K$, $g=2.57$, $\lambda=15.0 K$ and $R=1.8 \times 10^{-6}$, where $R = \sum(\chi_M T_{\text{cald}} - \chi_M T_{\text{obsd}})^2 / (\chi_M T_{\text{obsd}})^2$. The alternation parameter α ($\alpha=|J_1/J_2|$) is greater than 1, demonstrating that the whole chain through the mixed triple bridges of polymer **1** exhibits the predominantly ferromagnetic coupling at this range of temperature.

The field-cooled (FC) and zero-field-cooled (ZFC) magnetization measurements were performed at 20 Oe in the 2–30 K (Fig. S3). Below 25 K, the FC curve shows an abrupt increase until it reaches saturation with decreasing temperature; while the ZFC curve exhibits a rounded maximum and falls below $T=24 K$. The FC and ZFC curves show a divergence below the critical temperature $T_c=24 K$. Both of the curves reveal irreversibility and bifurcation, indicating the long-range magnetic ordering [16].

The field dependence of magnetizations shows rapid saturation of the M at ca. 20 kOe which are quite typical for long-range ferromagnetic ordering (Fig. S4). The nearly saturated magnetization value of 1.98 $N\beta$ at 50 kOe corresponds to the theoretical value for a ferromagnetic Ni $_2$ ($g=2$) system which is predicted by the Brillouin equation with $S=1$ for non-interacting molecules. The hysteresis loop at 2 K shows that the coercive field (H_c) is 3010 Oe

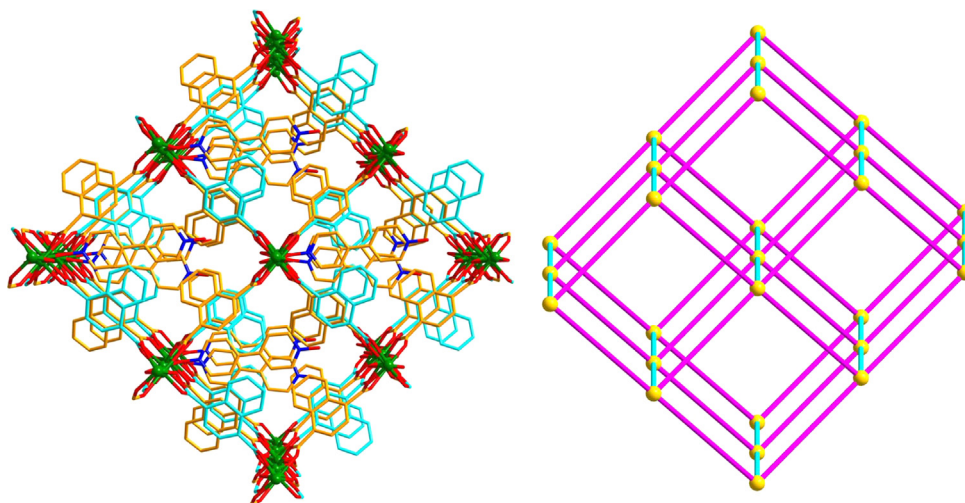


Fig. 3. Crystal structure of **1** showing the 3D framework with oxygen-bridged Ni-chains (left); the topological structure of **1** in which the pink bonds represent 1,4-NDC²⁻ ligands, the nodes represent [Ni1–O1W–Ni2] segments and the turquoise bonds represent the bridge of O2 (right).

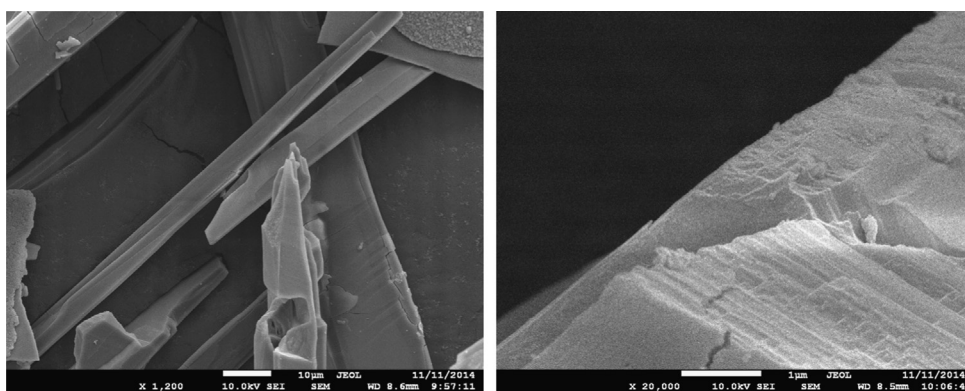


Fig. 4. SEM micrographs of the sample at different magnifications: 1200 (left) and 20000 (right).

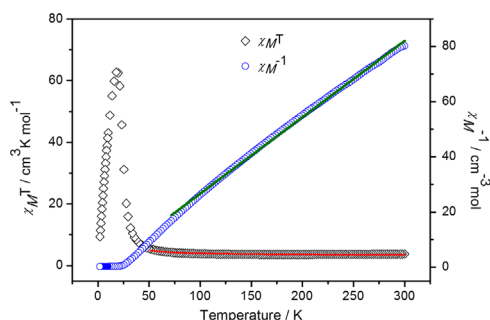


Fig. 5. Temperature dependence of $\chi_M T$ and inverse molar susceptibility χ_M^{-1} for **1**. The green line is the fit to Curie-Weiss expression, as described in the text, and the red line is the fit to the alternating 1D Heisenberg Fisher model.

and the remnant magnetization (M_R) is $0.94 N\beta$, which are in agreement with a soft-magnetic behavior.

3.4. Thermogravimetric analysis

The TG property of **1** was measured under air atmosphere with a heating rate of $10\text{ }^\circ\text{C min}^{-1}$ from 25 to $1000\text{ }^\circ\text{C}$ (Fig. S5). Polymer **1** loses weight gradually until $260\text{ }^\circ\text{C}$ corresponding to H_2O molecules with the value of 8.84% (caclcd. 8.93%) and continues loss from the decomposition of skeleton even at the upper limit of measurement range.

4. Conclusion

In summary, a 3D nickel(II) coordination polymer using two mixed ligands has been structurally and magnetically characterized. The magnetic behavior of **1** indicates it is a ferromagnetic framework with long-range magnetic ordering. Theoretical results also afford a satisfactory agreement with the observations. The assembly of these kinds of polymers is controllable, and can enrich the magnetic materials on polymers with long-range order.

Acknowledgments

This work was supported by the National Natural Science Foundation of China, Innovation Scientists and Technicians Troop Construction Projects of Henan Province, the Natural Science Foundation of Henan Province and the Foundation Co-established by the Province and the Ministry of Henan University.

Appendix A. Supporting information

Supplementary data associated with this article can be found in the online version at <http://dx.doi.org/10.1016/j.matlet.2014.11.127>.

References

- [1] Yaghi OM, O'Keeffe M, Ockwig NW, Chae HK, Eddaoudi M, Kim J. *Nature* 2003;423:705–14.
- [2] Rajkumar T, Ranga Rao G. *Mater Lett* 2008;62:4134–6.
- [3] Xuan S, Zhang Y, Zhou Y, Jiang W, Gong X. *J Mater Chem* 2012;22:13395–400.
- [4] Fei P, Zhong M, Lei Z, Su B. *Mater Lett* 2013;108:72–4.
- [5] Mounkachi O, El Moussaoui H, Masrour R, Ilali J, El Mediouri K, Hamedoun M, et al. *Mater Lett* 2014;126:193–6.
- [6] Clemente-Juan JM, Coronado E, Mínguez Espallargas G, Adams H, Brammer L. *Cryst Eng Comm* 2010;12:2339–42.
- [7] Xu W, Zhou Y, Huang D, Xiong W, Su M, Wang K, et al. *Cryst Growth Des* 2013;13:5420–32.
- [8] Yang C-I, Wernsdorfer W, Lee G-H, Tsai H-L. *J Am Chem Soc* 2006;129:456–7.
- [9] Zhang XM, Wang YQ, Li XB, Gao EQ. *Dalton Trans* 2012;41:2026–33.
- [10] Manna SC, Zangrando E, Ribas J, Ray Chaudhuri N. *Dalton Trans* 2007:1383–91.
- [11] An B, Bai Y, Wang J-L, Dang D-B. *Dalton Trans* 2014;43:12828–31.
- [12] An B, Zhou RM, Dang DB, Wang JL, Pan H, Bai Y. *Spectrochim Acta A. Mol Biomol Spectrosc* 2014;122:392–9.
- [13] Li H, An B, Bai Y, Wang J, Pan H, Dang D. *Syn Met* 2014;194:126–31.
- [14] Wang YQ, Sun WW, Wang ZD, Jia QX, Gao EQ, Song Y. *Chem Commun (Camb)* 2011;47:6386–8.
- [15] Zheng YZ, Qin L, Zheng Z, Xue W, Chen XM. *Dalton Trans* 2013;42:1770–7.
- [16] Gu Z-G, Xu Y-F, Yin X-J, Zhou X-H, Zuo J-L, You X-Z. *Dalton Trans* 2008:5593–602.